

# Hydrothermally Grown ZnO Nanoparticles for Photodegradation of Textile Dye

Bhawna<sup>1</sup>, Bishnu Pada Majee<sup>1</sup>, Vishal Choudhary<sup>1</sup>, Rajiv Prakash<sup>1</sup> and Ashish Kumar Mishra<sup>1,a)</sup>

<sup>1</sup>*School of Materials Science and Technology, Indian Institute of Technology (BHU), Varanasi, UP-221005, INDIA*

<sup>a)</sup>Corresponding author: ak Mishra.mst@iitbhu.ac.in

**Abstract.** Zinc oxide (ZnO) is one of the most investigated semiconductor material for photocatalytic applications such as solar cell, light emitting diode, photodiodes, photodetectors and sensors. Surface to volume ratio for nanoparticles increases with decrease in size and give rise to enhanced surface reactivity. Out of all available methods for the synthesis of ZnO nanoparticles hydrothermal method is one of the simplest methods with tolerable growth conditions. In the present work, hydrothermally grown ZnO nanoparticles have been demonstrated for photocatalytic degradation of direct violet dye, which is largely used in textile industries and hence can be found in industrial waste water. The synthesized ZnO nanoparticles have been characterized using SEM, X-ray diffraction, Raman and UV-Vis absorption spectroscopy. The average crystallite size as calculated using Scherrer formula comes out to be around 40 nm. The UV-Vis absorption spectrum of ZnO shows a sharp absorption band edge around 360 nm, indicating its UV responsive photocatalytic activity. Since direct violet dye is having an absorption in similar UV region, ZnO have been demonstrated for photocatalytic reduction of different concentrations of direct violet. It is observed that the photocatalytic process obey first order kinetics in the present work.

## INTRODUCTION

Wastewater outputs from the textile industry are contaminated with dyes and other organic compounds. Due to their carcinogenic nature and toxic behavior they pose serious health hazards and environmental issues to human society and hence removal of such dyes is a concern for our society [1-6]. Most of the existing methods generate secondary pollutants while treating waste water. As one of the effective methods, nanosized semiconductor photocatalyst are used to remove the dyes from wastewater. ZnO is non toxic, abundant in nature and possess high photocatalytic efficiency due to presence of direct band gap of 3.37eV, which is a function of particle size. Hence, ZnO nanoparticles are quite efficient for photodegradation of dyes. Nanostructured ZnO is highly demanded and considered as a multifunctional metal oxide because of its optical and electronic properties which are quite different from its bulk counterpart. They can also be efficiently operated at moderate conditions and reused effectively compared to other metal oxides [7-9]. Among three possible crystal structures of ZnO (hexagonal wurtzite, cubic zinc blende and rocksalt), hexagonal structure is most stable. There are several techniques to synthesize Nanostructured ZnO which includes wet chemical route, chemical vapor deposition, pulsed laser deposition and hydrothermal method. Different synthesis routes results in a wide range of morphologies like nanorods, nanobelts, flower-like, nanowires, nanosphere, cage-like and nanosaws [10-12]. Above mentioned morphologies can be achieved by tuning the synthesis conditions of the process.

In the present work, ZnO nanoparticles have been demonstrated for photocatalytic degradation of direct violet dye, which are largely used in textile industries for coloring purpose. ZnO nanoparticles of average size 40 nm have been synthesized by hydrothermal process. Morphological, structural and optical properties of synthesized ZnO have been analyzed using different characterization tools. Since the direct violet dye and ZnO nanoparticles have their absorption in similar UV region, ZnO has been used for its degradation. The degradation has been performed under UV radiation and kinetic study for the same has been performed.

## EXPERIMENT

Zinc acetate dehydrate [ $\text{Zn}(\text{CH}_3\text{COO})_2 \cdot 2\text{H}_2\text{O}$ ], MW 219.50 g/mol, 98.5% pure was obtained from Sisco Research Laboratories Pvt. Ltd., India. Methanol [ $\text{CH}_3\text{OH}$ ], MW 32.04 g/mol, 99.5% pure was purchased from Loba Chemie Pvt. Ltd., India. Direct violet dye, which is used in small textile industries at the banks of river Ganga, was bought from a local shop in Varanasi, India. These chemicals were used without further purification. In synthesis process, (0.2 M) solution of Zinc acetate dehydrate was prepared in 50 ml methanol. The reaction mixture was stirred magnetically for 30 minutes at room temperature and then transferred into Teflon lined sealed stainless steel autoclave of 100 ml capacity. It was then placed inside a preheated hot air oven which was maintained at 150°C for 6 hours. The furnace was allowed to cool naturally after the desired time. The resultant product was centrifuged, air dried for 2 hours.

Synthesized ZnO nanoparticles were characterized using X-ray diffraction, SEM, Raman and UV-vis absorption spectroscopy. Aqueous solutions of direct violet dye of different initial concentration (200, 100, 50, 25, 12.5 & 6.5 ppm) were prepared by serial dilution method to obtain a calibration curve for finding concentration of dye in treated solution. For photodegradation purpose, 40 ml of different dye solutions (200, 100 & 50 ppm) have been treated with 40 mg of ZnO separately under UV radiation for certain time period (up to 60 minutes). Concentration of residual dye content in treated aqueous dye solutions have been further studied using UV-vis absorption spectroscopy.

## RESULT AND DISCUSSION

The structural characterization of the hydrothermally synthesized ZnO nanoparticles was carried out using a table top, room temperature powder X-ray diffractometer (XRD, Rigaku MiniFlex 300/600 Japan) with  $\text{Cu K}_\alpha$  radiation at a wavelength of 1.54 Å. Diffraction data was collected over a  $2\theta$  range of 20° to 85°. Figure 1(a) shows the XRD pattern of synthesized ZnO nanoparticles. The diffraction peaks matched well with JCPDS file number 03-065-3411 and the pattern was indexed accordingly. It was observed that the synthesized nanoparticles exhibit crystalline hexagonal wurtzite structure. The average crystallite size of the ZnO nanoparticles was calculated using Scherrer's formula [13].

$$D = \frac{0.9\lambda}{\beta \cos \theta} \quad (1)$$

Where  $\lambda$  is the wavelength of X-ray radiation,  $\beta$  is the full width at half maxima (FWHM),  $\theta$  is the Bragg's angle and  $D$  is the crystallite size. For this purpose, three high intensity peaks (101), (100 and (002) peaks were chosen and the average crystallite size was found to be around 40±2 nm. Absence of any impurity peak also indicates the purity of the synthesized ZnO. The morphology of synthesized ZnO nanoparticles was observed using a scanning electron microscope (SEM, NovaNanoSEM 450). Figure 1(b) represents the SEM image of ZnO which indicates that the near spherical shape of grown ZnO. SEM image also shows that the synthesized ZnO nanoparticles are well separated, which reduces the possibility of agglomeration and hence better photocatalytic property can be achieved for ZnO. The scale value of SEM image indicates the average diameter of near spherical nanoparticles to be in the range of 35- 45 nm.

Raman study of as grown ZnO nanoparticles was performed with STR-300 Micro Raman Spectrometer (Airix Corp.) equipped with 532 nm green laser. The scattered light was collected in backscattering geometry with 1200 grating having instrumental error of around 1.2  $\text{cm}^{-1}$ . Figure 2 (a) represent the Raman spectra of ZnO nanoparticles. It shows an intense mode  $E_2^{\text{low}}$  at around 99  $\text{cm}^{-1}$ , which is attributed to the vibrations of zinc sublattice in ZnO. Another intense Raman mode is  $E_2^{\text{high}}$  at around 437  $\text{cm}^{-1}$ , which is assigned to oxygen vibrations. The peak at around 330  $\text{cm}^{-1}$  is the second order Raman mode and ascribed to the difference  $E_2^{\text{high}} - E_2^{\text{low}}$ . In addition to these strong peaks, two weak signals can be seen around 385 and 410  $\text{cm}^{-1}$ , which belongs to polar  $A_1(\text{TO})$  and  $E_1(\text{TO})$ , respectively. Similarly, a weak peak around 660  $\text{cm}^{-1}$  indicates the TA+LO mode in ZnO nanoparticles. Presence of all these peaks clearly indicates the formation of wurtzite ZnO nanostructure as described in literature [14]. The UV-vis absorption spectroscopy was performed with UV-vis spectrophotometer (BioTek) over a wavelength range of 200 nm to 850 nm. Aqueous dispersion of synthesized nanoparticles was prepared for this purpose. Figure 2(b) represents the plot between absorbance and wavelength of hydrothermally grown ZnO nanoparticles. A sharp

absorption band edge was observed around 360 nm, indicating the UV responsive photocatalytic activity of synthesized ZnO nanoparticles. Further, band gap was calculated using the Tauc equation-

$$(\alpha h\nu)^2 = A(h\nu - E_g) \quad (2)$$

where  $\alpha$  is the absorption coefficient of the material,  $h\nu$  is the energy of incident light and  $E_g$  is the optical band gap of the material. The band gap of synthesized nanoparticles of ZnO was estimated by extrapolating the linear portion of the  $(\alpha h\nu)^2$  vs  $h\nu$  graph till it cut the x-axis as shown in inset of Fig. 2(b). The value of band gap was found to be around 3.18 eV.

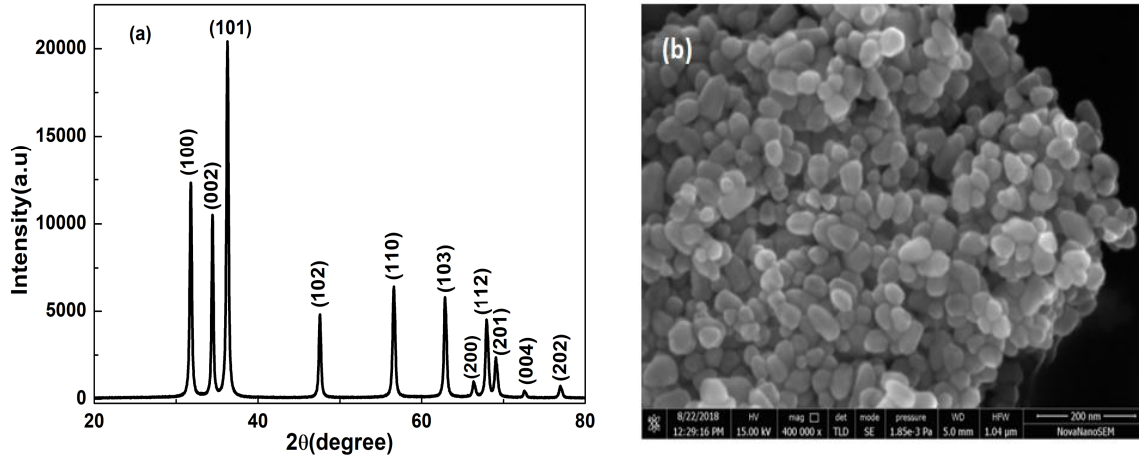


FIGURE 1.(a)XRD pattern, (b)SEM image of synthesized ZnO nanoparticles.

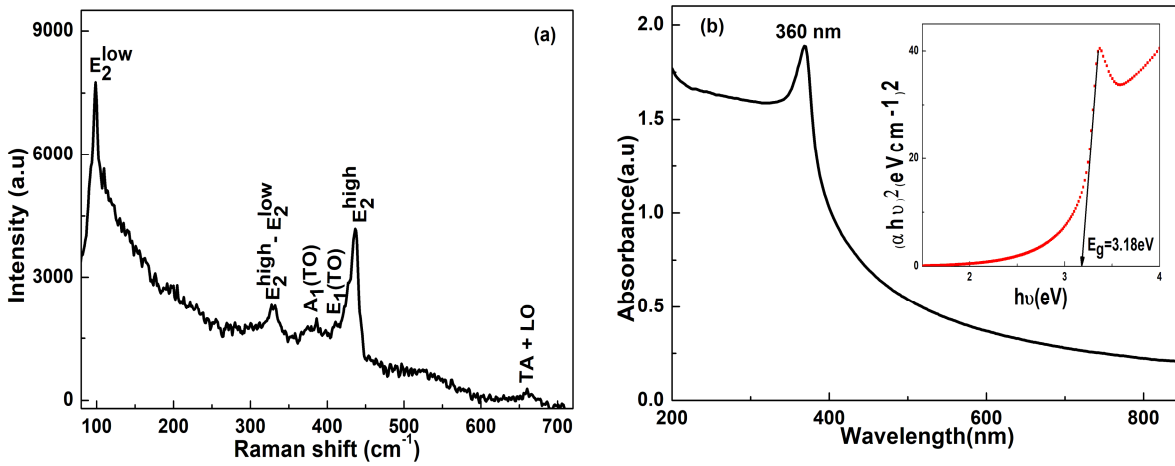
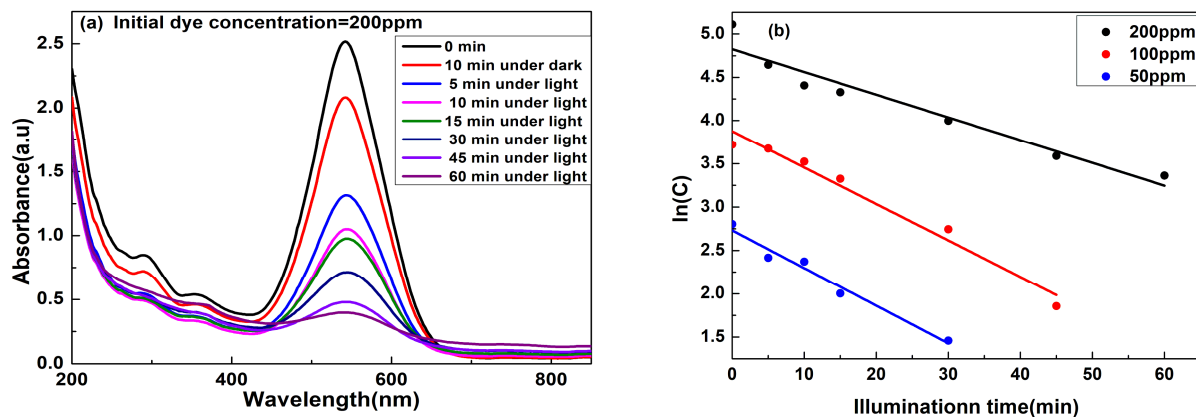


FIGURE 2.(a)Raman spectra, (b) UV-vis absorption spectra with inset Tauc plot for synthesized ZnO nanoparticles.



**FIGURE 3.**(a)UV-Visible spectra of treated direct violet dye of 200 ppm initial concentration,(b)pseudo first order kinetics of dye with initial concentration equal to 200,100 and 50 ppm.

Further photocatalytic degradation of direct violet dye is performed for 200, 100 and 50 ppm aqueous dye solution (40 ml) separately in 100 ml quartz tube inside the indigenously designed UV chamber having four UV lamps of 8 W power. Initially, 40 mg of ZnO nanoparticles were dispersed in the dye solution of quartz tube and kept for 10 min in dark and then illuminated with UV light. While being irradiated with UV light the quartz tube having dye solution was continuously rotated for uniform illumination throughout the solution. At every particular time interval, 2 ml of irradiated solution was collected and their absorption spectra were recorded to observe the residual dye concentration.

The UV-vis absorption spectra of photodegraded 200 ppm direct violet dye solution with ZnO nanoparticles is shown in fig. 3a. Similar curves were obtained for 100 and 50 ppm dye solution and corresponding dye concentrations were calculated. The degradation kinetics was studied using pseudo first order equation-

$$\ln(C) = \ln(C_0) - kt \quad (3)$$

where  $k$  is the reaction rate constant,  $C_0$  is the initial concentration of aqueous direct violet dye,  $C$  is the concentration of dye after irradiation time  $t$ . Applying equation (3), curves for  $\ln(C)$  vs  $t$  were plotted for photodegraded aqueous dye solutions, as shown in Fig 3(b). A linear fit was observed indicating that the photocatalytic degradations of direct violet dye using ZnO nanoparticles follow pseudo first order kinetics. The rate constants for photocatalytic process were obtained as 0.026, 0.042 and 0.043  $\text{min}^{-1}$  for 200, 100 and 50 ppm, respectively. This indicates that photodegradation rate of direct violet dye decreases largely from 100 ppm solution to 200 ppm solution. This was attributed to the fact that with increase in dye concentration the ratio of dye molecules to the ZnO nanoparticles increases, which in turn effectively decreases the probability of electron-hole pair formation in ZnO and hence decreasing the photocatalytic activity of the synthesized ZnO nanoparticles.

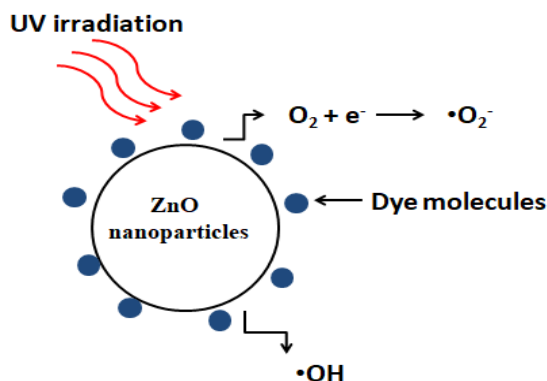


**FIGURE 4.** Schematic of mechanism involved in photodegradation of dye by ZnO nanoparticles.

The mechanism involved in the photocatalytic degradation of direct violet dye using ZnO nanoparticles is shown in Fig. 4. Upon being photoexcited with UV radiation, coming from a light source or sunlight, there is generation of

electron-hole pair on or near the surface of the photocatalyst (in this case ZnO nanoparticles) due to the transfer of electron from valence band to the conduction band. These photogenerated electron-hole pair can quickly recombine to generate heat. If there exist any chemical species adsorbed on to the surface of photocatalyst then they can capture these charge carriers and reduce the possibility of recombination. When the water or hydroxyl anions that are adsorbed on the surface react with the valence band hole they generate hydroxyl radicals. Also reaction of atmospheric or dissolved oxygen with the conduction band electron generates superoxide radicals [15]. Due to their high reactivity these radicals attack the adsorbed direct violet dye and degrade them under the illumination.

## CONCLUSION

ZnO nanoparticles were grown by hydrothermal method and characterized by XRD, SEM, Raman and UV-visible spectroscopy techniques. The obtained results confirmed the successful formation of nano sized ZnO particles. The photocatalytic activity of synthesized ZnO nanoparticles was evaluated by degrading the aqueous solution of direct violet dye, which is largely used in textile industries. The photocatalytic degradation process follows pseudo first order kinetics and the degradation rate is affected with increasing dye concentration and appropriate mechanism has been discussed. This process helps to develop methods for treatment of textile waste water without generation of any secondary pollutants.

## ACKNOWLEDGMENTS

The authors thank the support of IIT BHU. Bhawna acknowledges the support of DST, India for INSPIRE fellowship. AKM acknowledges the support of SERB and DST, India for grants no.ECR/2017/000558 and IFA14-MS25.

## REFERENCES

1. A. Ahmad and J. Walsh, *J. Mater. Sci.* **38**, 4325–4332(2003).
2. M.H.Habibi and M.H.Rahmati, *Spectrochim. Acta A.* **137**, 160–164(2015).
3. R. Saleh and N.F.Djaja, *Spectrochim. Acta A.* **130**, 581–590(2014).
4. S. Ito, T.N. Murakami, P. Comte, P. Liska, C. Grätzel, M.K. Nazeeruddin and M. Grätzel, *Thin Solid Films* **516**, 4613–4619(2008).
5. S. Baruah and J. Dutta, *Sci. Technol. Adv. Mater.* **10** (2009) 013001.
6. R. Kant, *Nat. Sci.* **4**, 22-26 (2012).
7. Y. Li, W. Xie, X. Hu, G. Shen, X. Zhou, Y. Xiang, X. Zhao and P. Fang, *Langmuir* **26**, 591–597(2009).
8. A.A. Al-Ghamdi, O.A. Al-Hartomy, M. ElOkr, A.M. Nawar, S. El-Gazzar, F. El-Tantawy, F. Yakuphanoglu, *Spectrochim. Acta A.* **131**, 512–517(2014).
9. L.F.M. Ismail, M.M. Emara, M.M. El-Moselhy, N.A. Maziad, O.K. Hussein, *Spectrochim. Acta A* **131**, 158–168(2014).
10. H.N. Tien, V.H. Luan, L.T. Hoa, N.T. Khoa, S.H. Hahn, J.S. Chung, E.W. Shin, S.H. Hur, *Chem. Eng J.* **229**, 126–133(2013).
11. B. Li, T. Liu, Y. Wang, Z. Wang, *J. Colloid Interf. Sci.* **377**, 114–121(2012).
12. M.M. Muñoz, J.E.R. Ibarra, J.E.R. Páez, A. Ramirez and J.A.H. Coaquira, *J. Phys.: Conf. Ser.* **792**(2017) 012068.
13. B. D. Cullity, *Elements of X-Ray Diffraction*, Addison-Wesley, 2001.
14. M. Scepanovic, M. Grujic-Brojcin, K. Vojisavljevic, S. Bernik and T. Sreckovic, *J. Raman Spectrosc.* **41**, 914–921(2010).
15. A.C. Dodd, A.J. McKinley, M. Saunders and T. Suzuki, *Journal of Nanoparticle Research* **8**, 43–51(2006).